Asian Journal of Chemistry; Vol. 37, No. 12 (2025), 3219-3228
ASIAN JOURNAL OF CHEMISTRY
https://doi.org/10.14233/ajchem.2025.34766

Synthesis and Evaluation of (2,5-Dimethylthiophen-3-yl)pyrimidin-2-amine Derivatives as Antidepressants by *In silico* and *In vivo* Methods

PALUPANURI NAVEENA and KONDA SWATHI*

Department of Pharmaceutical Chemistry, Institute of Pharmaceutical Technology, Sri Padmavati Mahila Visvavidyalayam, Tirupati-517502, India

*Corresponding author: E-mail: kswathi84@yahoo.co.in

Received: 25 July 2025 *Accepted*: 28 November 2025 *Published online*: 30 November 2025 AJC-22214

The present study involves the design, synthesis, *in silico* evaluation and biological assessment of a new series of (2,5-dimethylthiophen-3-yl)pyrimidin-2-amine derivatives (**4a7-4h7**) as potential antidepressant agents. The synthesis followed a two-step route first, (2,5-dimethyl-thiophen-3-yl)prop-2-en-1-one derivatives (**4a-7**) were synthesized *via* Claisen–Schmidt condensation, followed by cyclization with guanidine to obtain the target pyrimidin-2-amine derivatives (**4a7-4h7**). The designed molecules were evaluated using Swiss-ADME,Molinspiration, Protox-II and SwissTargetPrediction to predict drug-likeness, ADME properties, toxicity and target profiles. All compounds satisfied Lipinski's rule of five and showed favourable pharmacokinetic and safety profiles. Molecular docking against the serotonin transporter (SERT, PDB ID: 1KUV) revealed that compounds **4e7** (Glide score -7.8) and **4h7** (Glide score -8.0) exhibited the strongest binding affinities, outperforming the reference drug imipramine. Molecular dynamics simulations using GROMACS further confirmed the stability of ligand–protein complexes, with compound **4h7** displaying excellent structural stability throughout the simulation. The synthesized derivatives were characterized by IR, ^{1}H NMR, ^{13}C NMR and mass spectroscopy. Their antidepressant potential was evaluated using the Forced Swim Test (FST) and Tail Suspension Test (TST) in mice, where compounds **4e7** and **4h7** significantly reduced immobility time, showing activity comparable to imipramine. Among all tested compounds, compound **4h7** demonstrated the highest level of potency.

Keywords: Thiophene, Pyrimidine, Docking studies, MD simulations, *In vivo* studies, Forced swim test, Tail suspension test.

INTRODUCTION

Pyrimidine is a privileged heterocyclic scaffold found in numerous bioactive molecules and clinically important drugs due to its electronic versatility, hydrogen-bonding ability and structural adaptability [1,2]. Over the past decades, pyrimidine derivatives have gained significant attention for their broad pharmacological spectrum, including anti-inflammatory, anticancer, antimicrobial, antidiabetic, antimalarial and other therapeutic applications [3-12]. This diversity highlights the importance of pyrimidine-based frameworks in modern medicinal chemistry.

Recent advancements in neuropharmacology have emphasized the relevance of pyrimidine derivatives in central nervous system (CNS) therapeutics, particularly for disorders associated with monoaminergic dysfunction such as depression. High-resolution structural elucidation of the human serotonin transporter (SERT) has offered critical insights into ligand–transporter interactions, facilitating rational design of serotonin modulating agents [13,14]. Several pyrimidine-based molecules have shown promising antidepressant activity through mechanisms involving selective serotonin reuptake inhibition (SSRI), multi-receptor interactions or kinase modulation [15-18]. Furthermore, hybrid heterocycles containing pyrimidine rings such as tetrazolo-pyrimidines, triazolo-pyrimidines and marine inspired analogues have demonstrated notable CNS activity, including antidepressant and anticonvulsant properties [19,20]. Incorporating electron-rich aromatic groups or sulfur containing moieties (*e.g.* thiophene) often enhances CNS penetration, improves receptor binding and modulates pharmacokinetic behaviour [21-23].

Based on this rationale, designing (2,5-dimethylthiophen-3-yl)pyrimidin-2-amine derivatives is a promising strategy for discovering new antidepressant agents. The thiophene ring can improve lipophilicity and CNS accessibility, while the pyrimidine nucleus serves as a well-established pharmaco-

phore for modulating neurotransmitter-related pathways. Integrating *in silico* techniques (molecular docking, receptor binding, ADMET prediction) with *in vivo* evaluations provides a powerful framework for identifying potential lead candidates.

Therefore, the present study aims to synthesize, computationally evaluate and biologically assess a new series of (2,5-dimethylthiophen-3-yl)pyrimidin-2-amine derivatives to explore their potential as novel antidepressants.

EXPERIMENTAL

All the laboratory grade solvents and chemicals, procured from the Sigma-Aldrich (USA), were utilized. The uncorrected melting points of the synthesized compounds were determined using a Mettler Toledo FP 62 melting point apparatus. Proton NMR (^{1}H NMR) spectra were obtained on a 500 MHz Bruker Avance DPX 200 NMR spectrometer operating in DMSO-d_6 solvent with TMS serving as the internal reference standard. Mass spectra were recorded using a Shimadzu QP2010 spectrometer equipped with a direct insertion probe at 70 eV. Analytical TLC analysis was carried out on silica gel G F_{254} plates.

Step-1: General method for synthesis of substituted 2,3-dimethyl thiophene prop-2-en-1-ones (4a-h): A stirred ethanolic solution of 3-acetyl-2,5-dimethylthiophene (0.01 M) was treated with an aqueous KOH solution (0.01 M) to generate the corresponding enolate intermediate under basic conditions. An equimolar quantity of the desired aromatic aldehyde was then introduced into this mixture, initiating a Claisen-Schmidt condensation reaction. The reaction was maintained at room temperature for 24 h, allowing the formation of α,β-unsaturated ketone structure characteristic of chalcone derivatives. Upon completion, reaction mixture was acidified using 1:1 HCl solution, resulting in precipitation of crude chalcone product (**Scheme-I**). The solid was separated by filtration, thoroughly washed with water and purified by recrystallization from methanol to obtain pure chalcone derivatives in good yield.

(2*E*)-3-(3,4-Dimethoxyphenyl)-1-(2,5-dimethylthiophen-3-yl)prop-2-en-1-one (4a): Colour: pale yellow solid, yield: 82%, m.p.: 166-168 ºC; IR (KBr, ν_{max}, cm^{-1}): 1710 (C=C), 784 (C–S), 1337 (C–CH_3), 1054 (C–O); ^{1}H NMR (500 MHz, DMSO-d_6, δ ppm): 7.98 (s, 1H), 7.08-6.95 (m, 3H), 6.91 (s, 1H), 6.85 (s, 1H), 3.82-3.76 (m, 6H), 2.44-2.40 (m, 3H), 2.35-2.31 (m, 3H); ^{13}C NMR (125 MHz, DMSO-d_6, δ ppm): 183.92 (s), 151.74 (s), 149.93 (s), 145.37 (s), 144.67 (s), 140.15 (s), 131.74 (s), 130.01 (s), 129.58 (s), 122.63 (s), 121.84 (s), 112.69 (s), 111.41 (s), 56.78 (s), 17.97 (s), 16.19 (s). MS: EIMS (*m/z*) 301 (M+1).

(2*E*)-1-(2,5-Dimethylthiophen-3-yl)-3-(3-nitrophenyl)-prop-2-en-1-one (4b): Colour: yellow solid, yield: 75%, m.p.: 180-182 ºC; IR (KBr, ν_{max}, cm^{-1}): 762 (C–S), 1450 (C–CH_3), 1736 (C=O), 1628 (C=C), 1511 (N–O), 1282 (C–N); ^{1}H NMR (500 MHz, DMSO-d_6, δ ppm): 8.32 (t, *J* = 1.4 Hz, 1H), 8.17-7.98 (m, 2H), 7.72 (dt, *J* = 7.5, 1.5 Hz, 1H), 7.51 (t, *J* = 7.5 Hz, 1H), 7.17 (d, *J* = 15.2 Hz, 1H), 7.07 (s, 1H), 2.41 (s,

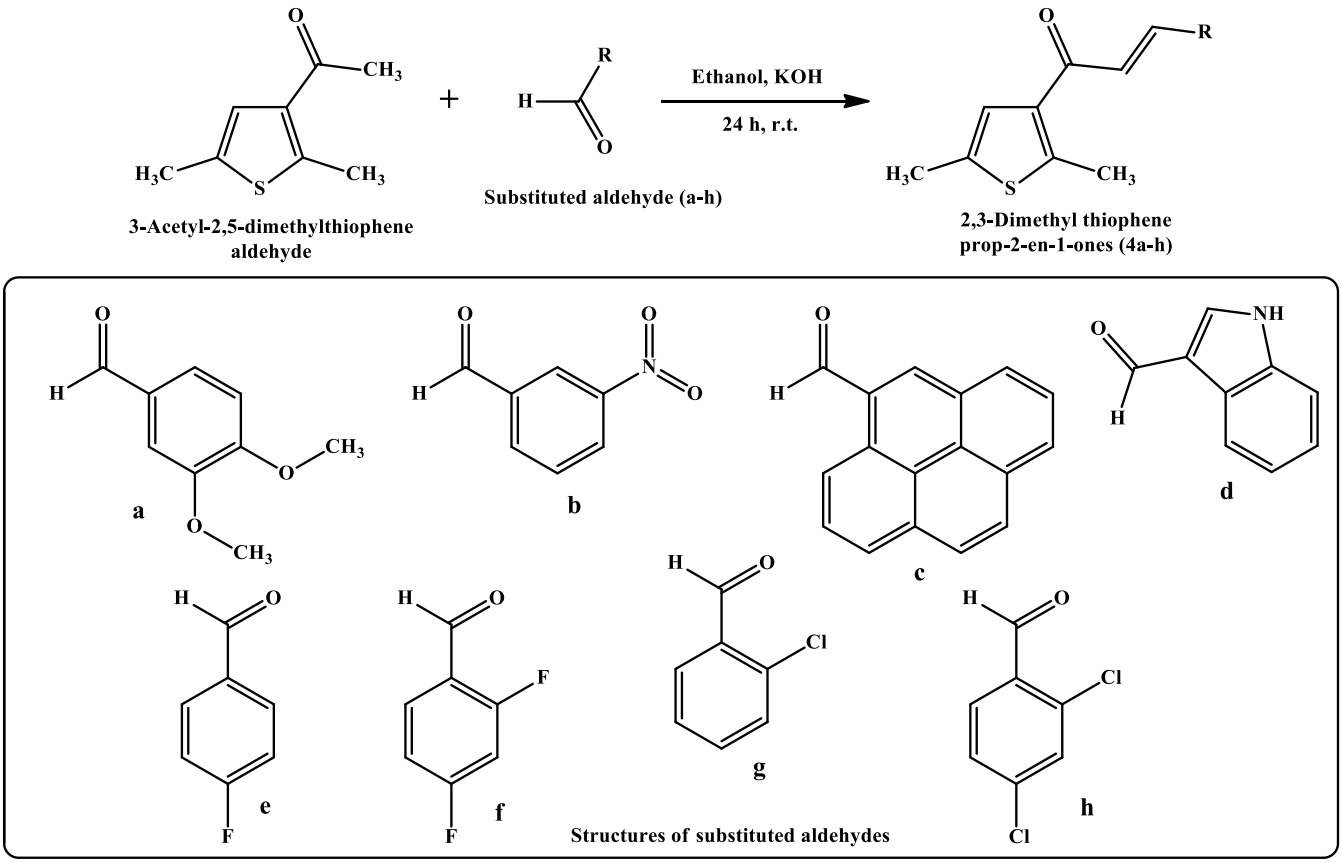

Scheme-I

3H), 2.34 (s, 3H); ^{13}C NMR (125 MHz, DMSO-d_6, δ ppm): 183.92 (s), 148.16 (s), 145.37 (s), 144.67 (s), 140.15 (s), 137.99 (s), 135.45 (s), 131.74 (s), 129.58 (s), 129.20 (s), 125.55 (s), 123.90 (s), 121.84 (s), 17.97 (s), 16.19 (s); MS: EIMS (*m/z*) 289 (M+1).

1-(2,5-Dimethylthiophen-3-yl)-3-(benzophenanthrenyl)-prop-2-en-1-one (4c): Colour: pale yellow solid, yield: 82%, m.p.: 140 ºC; IR (KBr, ν_{max}, cm^{-1}): 761 (C–S), 1312 (C–CH_3), 1732 (C=O), 1627 (C=C), 2937 (C–H); ^{1}H NMR (500 MHz, DMSO-d_6, δ ppm): 7.64 (d, *J* = 15.2 Hz, 1H), 7.03 (s, 1H), 6.42-6.35 (m, 2H), 6.35-6.19 (m, 3H), 5.93-5.84 (m, 3H), 3.14 (dd, *J* = 11.8, 0.7 Hz, 1H), 3.07 (d, *J* = 11.7 Hz, 1H), 2.34 (d, *J* = 15.8 Hz, 6H), 2.19-1.62 (m, 4H); ^{13}C NMR (125 MHz, DMSO-d_6, δ ppm): 184.88 (s), 150.08 (s), 148.69 (s), 145.66 (s), 145.37 (s), 143.21 (s), 140.15 (s), 138.28 (s), 137.73 (s), 134.31 (s), 131.74 (s), 130.13 (d, *J* = 12.4 Hz), 127.57 (s), 124.52 (s), 124.06 (s), 123.61 (s), 121.84 (s), 119.78 (s), 54.51 (s), 53.13-30.37 (m), 32.37-30.37 (m), 17.97 (s), 16.19 (s). MS: EIMS (*m/z*) 372 (M+1).

(2*E*)-1-(2,5-Dimethylthiophen-3-yl)-3-(1*H*-indol-3-yl)-prop-2-en-1-one (4d): Colour: pale yellow solid, yield: 80%, m.p.: 130-132 ºC; IR (KBr, ν_{max}, cm^{-1}): 1627 (C=C), 761 (C–S), 1312 (C–CH_3), 3464 (NH), ^{1}H NMR (500 MHz, DMSO-d_6, δ ppm): 7.66 (s, 1H), 7.54 (d, *J* = 15.2 Hz, 1H), 7.35-7.07 (m, 5H), 6.99 (d, *J* = 15.0 Hz, 1H), 2.49 (s, 3H), 2.34 (s, 3H); ^{13}C NMR (125 MHz, DMSO-d_6, δ ppm): 184.88 (s), 145.37 (s), 140.15 (s), 136.55 (s), 135.06 (s), 132.68 (s), 131.74 (s), 129.26 (s), 123.96 (s), 121.83 (d, *J* = 3.7 Hz), 121.16 (s), 120.08 (s), 118.42 (s), 112.56 (s), 17.97 (s), 16.19 (s). MS: EIMS (*m/z*) 282 (M+1).

(2*E*)-1-(2,5-Dimethylthiophen-3-yl)-3-(4-fluorophenyl)-prop-2-en-1-one (4e): Colour: white solid, yield: 78%, m.p.: 119-120 ºC; IR (KBr, ν_{max}, cm^{-1}): 732 (C–S), 1238 (C–F), 1551 (C=C), 1680 (C=O), 1464 (C–CH_3); ^{1}H NMR (500 MHz, DMSO-d_6, δ ppm): 8.01 (d, *J* = 15.0 Hz, 1H), 7.50-7.16 (m, 2H), 7.07 (s, 1H), 7.00 (t, *J* = 7.8 Hz, 2H), 6.92 (d, *J* = 15.0 Hz, 1H), 2.42 (s, 3H), 2.34 (s, 3H); ^{13}C NMR (125 MHz, DMSO-d_6, δ ppm): 183.92 (s), 164.63 (s), 162.53 (s), 145.37 (s), 144.19 (s), 140.15 (s), 133.11 (d, *J* = 3.7 Hz), 131.74 (s), 130.28 (d, *J* = 6.7 Hz), 128.41 (s), 121.84 (s), 115.62 (s), 115.40 (s), 17.97 (s), 16.19 (s). MS: EIMS (*m/z*) 261 (M+1).

(2*E*)-3-(2,4-Difluorophenyl)-1-(2,5-dimethylthiophen-3-yl)prop-2-en-1-one (4f): Colour: pale yellow solid, yield: 76%, m.p.: 126-128 ºC; IR (KBr, ν_{max}, cm^{-1}): 755 (C–S), 1412 (C–CH_3), 1642 (C=C), 1340 (C–F), ^{1}H NMR (500 MHz, DMSO-d_6, δ ppm): 8.12 (d, *J* = 15.2 Hz, 1H), 7.31 (dt, *J* = 7.4, 5.0 Hz, 1H), 7.07 (s, 1H), 6.83-6.54 (m, 3H), 2.46 (s, 3H), 2.33 (s, 3H); ^{13}C NMR (125 MHz, DMSO-d_6, δ ppm): 183.92 (s), 164.93 (d, *J* = 7.6 Hz), 162.83 (d, *J* = 6.7 Hz), 162.08 (d, *J* = 6.7 Hz), 159.98 (d, *J* = 7.6 Hz), 145.37 (s), 140.15 (s), 137.72 (d, *J* = 6.7 Hz), 132.20-131.63 (m), 121.84 (s), 118.94 (d, *J* = 3.7 Hz), 118.73 (d, *J* = 3.7 Hz), 113.11 (d, *J* = 3.7 Hz), 112.89 (d, *J* = 3.7 Hz), 103.73 (s), 103.51 (s), 103.29 (s), 17.97 (s), 16.19 (s); MS: EIMS (*m/z*) 279 (M+1).

(2*E*)-3-(2-Chlorophenyl)-1-(2,5-dimethylthiophen-3-yl)-prop-2-en-1-one (4g): Colour: white solid, yield: 78%, m.p.: 110-112 ºC; IR (KBr, ν_{max}, cm^{-1}): 622 (C–S), 815 (C–Cl), 1641 (C=O), 1612 (C=C), 1369 (C–CH_3); ^{1}H NMR (500 MHz, DMSO-d_6, δ ppm): 8.33 (d, *J* = 15.0 Hz, 1H), 7.47-7.22 (m, 2H), 7.20-7.09 (m, 2H), 7.07 (s, 1H), 6.83 (d, *J* = 15.2 Hz, 1H), 2.43 (s, 3H), 2.34 (s, 3H); ^{13}C NMR: (125 MHz, DMSO-d_6, δ ppm): 183.92 (s), 145.37 (s), 140.15 (s), 137.83 (s), 133.22 (s), 132.70 (s), 131.94 (s), 131.74 (s), 131.06 (s), 130.16 (s), 128.62 (s), 127.33 (s), 121.84 (s), 17.97 (s), 16.19 (s). MS: EIMS (*m/z*) 277 (M+1).

(2*E*)-3-(2,4-Dichlorophenyl)-1-(2,5-dimethylthiophen-3-yl)prop-2-en-1-one (4h): Colour: pale yellow solid, yield: 81%, m.p.: 112-115 ºC; IR (KBr, ν_{max}, cm^{-1}): 758 (C–S), 1352 (C–CH_3), 1667 (C=C), 1748 (C=O), 593 (C–Cl); ^{1}H NMR (500 MHz, DMSO-d_6, δ ppm): 8.31 (d, *J* = 15.2 Hz, 1H), 7.35 (d, *J* = 1.4 Hz, 1H), 7.26 (d, *J* = 7.5 Hz, 1H), 7.17 (dd, *J* = 7.5, 1.4 Hz, 1H), 7.07 (s, 1H), 6.81 (d, *J* = 15.0 Hz, 1H), 2.42 (s, 3H), 2.33 (s, 3H); ^{13}C NMR (125 MHz, DMSO-d_6, δ ppm): 183.92 (s), 145.37 (s), 140.15 (s), 137.83 (s), 135.74 (s), 134.60 (s), 132.04-131.63 (m), 131.18 (s), 129.85 (s), 128.18 (s), 121.84 (s), 17.97 (s), 16.19 (s); MS: EIMS (*m/z*) 312 (M+1).

Step-2: General synthetic method of (2,5-dimethylthiophen-3-yl)prop-2-en-1-one derivatives (4a7-4h7): A mixture of 1,3-diarylprop-2-en-1-ones (**4a-h**, 0.01 M) and guani-dine hydrochloride was dissolved in 25 mL ethanol and KOH (0.01 M) was added to promote the cyclization under basic conditions. The reaction mixture was refluxed on a water bath for approximately 6 h at 180 ºC, enabling the nucleophilic addition followed by ring closure to yield substituted pyrimidine derivatives. Upon completion, the excess solvent was evaporated under reduced pressure and the resulting crude residue was purified through column chromatography using a suitable solvent system, affording the desired thiophene-pyrimidine hybrid derivatives (**4a7-4h7**) in pure form (**Scheme-II**).

4-(3,4-Dimethoxyphenyl)-6-(2,5-dimethylthiophen-3-yl)pyrimidin-2-amine (4a7): Colour: yellow solid, yield: 78%, m.p.: 124-126 ºC; IR (KBr, ν_{max}, cm^{-1}): 758 (C–S), 1611 (C=C), 1352 (C–CH_3), 1667 (C=N), 1213 (C–N), 3467 (NH_2), ^{1}H NMR (500 MHz, DMSO-d_6, δ ppm): 7.57-7.29 (m, 3H), 7.26 (s, 1H), 7.04 (d, *J* = 7.5 Hz, 1H), 3.80 (s, 6H), 2.51 (s, 2H), 2.47 (d, *J* = 44.3 Hz, 5H), 2.35 (s, 3H). ^{13}C NMR: (125 MHz, DMSO-d_6, δ ppm): 161.05 (s), 157.92 (s), 155.06 (s), 152.54 (s), 149.88 (s), 140.44 (s), 138.64 (s), 131.60 (s), 130.98 (d, *J* = 11.4 Hz), 122.87 (s), 115.51 (s), 113.21 (s), 107.91 (s), 56.78 (s), 17.97 (s), 16.65 (s). MS: EIMS (*m/z*) 342 (M+1).

4-(2,5-Dimethylthiophen-3-yl)-6-(3-nitrophenyl)pyrimidin-2-amine (4b7): Colour: white solid, yield: 72%, m.p.: 153-155 ºC; IR (KBr, ν_{max}, cm^{-1}): 1667 (C=N), 1437 (N–O), 1213 (C–N), 758 (C–S), 1352 (C–CH_3), 3012 (NH_2); ^{1}H NMR (500 MHz, DMSO-d_6, δ ppm): 8.32 (t, *J* = 1.4 Hz, 1H), 8.17-7.98 (m, 2H), 7.72 (dt, *J* = 7.5, 1.5 Hz, 1H), 7.51 (t, *J* = 7.5 Hz, 1H), 7.17 (d, *J* = 15.2 Hz, 1H), 7.07 (s, 1H), 2.41 (s, 3H), 2.34 (s, 3H); ^{13}C NMR (125 MHz, DMSO-d_6, δ ppm): 161.05 (s), 157.92 (s), 155.06 (s), 149.46 (s), 141.28 (s), 140.44 (s), 138.64 (s), 137.64 (s), 131.60 (s), 131.02 (s), 129.00 (s), 127.69 (s), 125.91 (s), 107.91 (s), 17.97 (s), 16.65 (s); MS: EIMS (*m/z*) 327 (M+1).

4-(2,5-Dimethylthiophen-3-yl)-6-(benzophenanthrenyl)-pyrimidin-2-amine (4c7): Colour: pale yellow solid, yield: 78%, m.p.: 140-142 ºC; IR (KBr, ν_{max}, cm^{-1}): 756 (C–S),

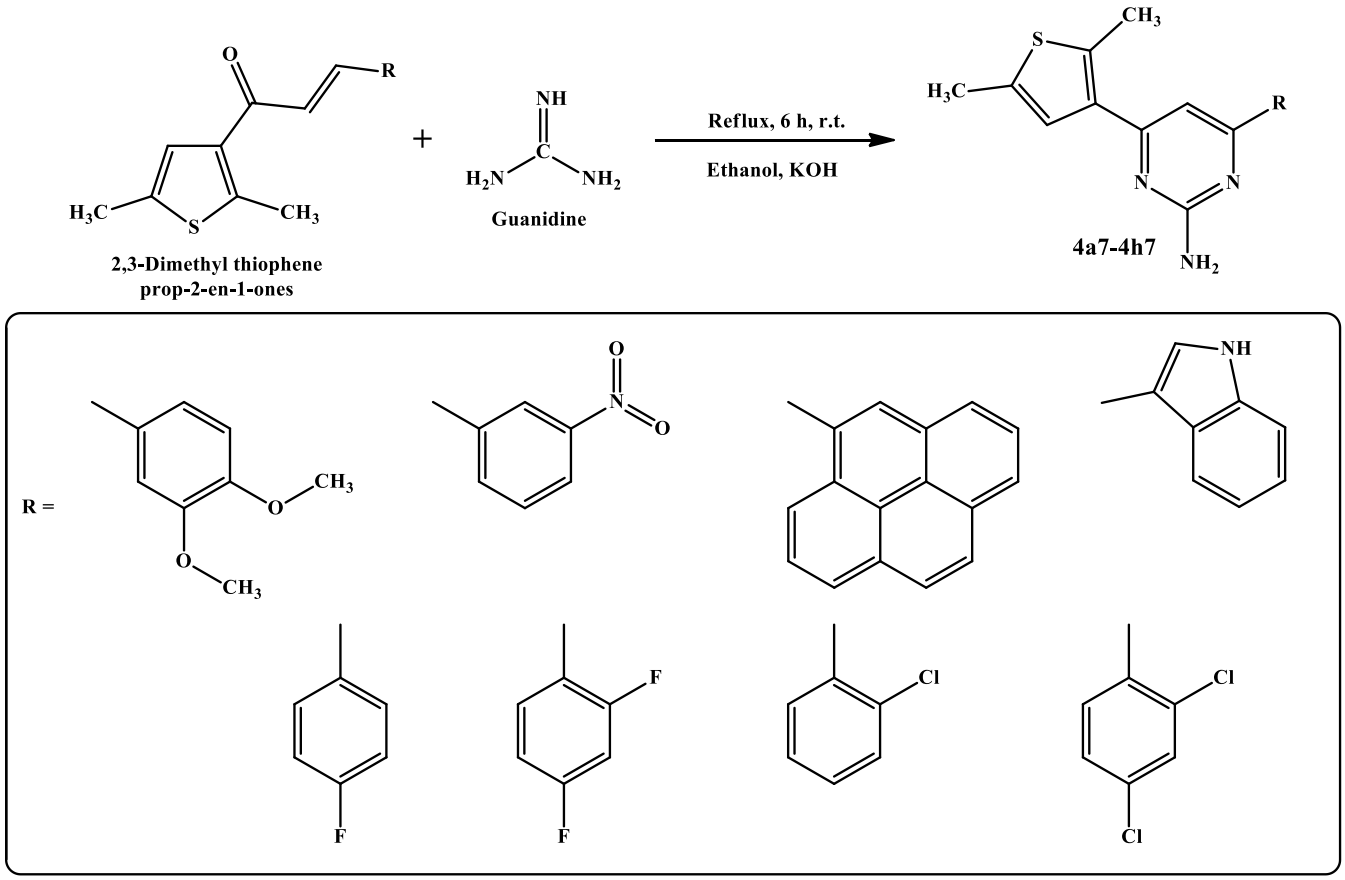

Scheme-II

1656 (C=C), 1354 (C–CH_3), 1610 (C=N), 3341 (NH_2), 3048 (C–H); ^{1}H NMR (500 MHz, DMSO-d_6, δ ppm): 8.02 (d, *J* = 1.6 Hz, 1H), 7.90-7.53 (m, 1H), 7.47-7.38 (m, 2H), 7.35 (s, 1H), 7.27 (s, 1H), 6.53-6.32 (m, 3H), 6.13 (dd, *J* = 11.0, 6.2 Hz, 1H), 4.41-3.84 (m, 1H), 3.33 (qdd, *J* = 12.2, 6.2, 0.6 Hz, 2H), 2.55 (s, 2H), 2.50 (d, *J* = 46.7 Hz, 5H), 2.35 (s, 3H); ^{13}C NMR (125 MHz, DMSO-d_6, δ ppm): 159.52 (s), 158.69 (s), 158.24 (s), 140.44 (s), 138.64 (s), 138.01 (s), 136.59 (s), 135.00 (s), 134.20 (s), 131.84 (d, *J* = 19.1 Hz), 131.60 (s), 131.02 (s), 129.64 (d, *J* = 12.4 Hz), 128.63 (s), 127.50 (s), 126.33 (s), 124.99 (s), 122.80 (s), 120.85 (s), 109.25 (s), 31.42 (s), 17.97 (s), 16.65 (s); MS: EIMS (*m/z*) 408 (M+1).

4-(2,5-Dimethylthiophen-3-yl)-6-(1*H*-indol-2-yl)pyrimidin-2-amine (4d7): Colour: red solid, yield: 70%, m.p.: 181-182 ºC; IR (KBr, ν_{max}, cm^{-1}): 875 (C–S), 1657 (C=C), 1336 (C–CH_3), 1624 (C=N), 3296 (NH_2), 1745 (NH); ^{1}H NMR (500 MHz, DMSO-d_6, δ ppm): 7.73 (dt, *J* = 7.3, 1.4 Hz, 21H), 7.64 (dd, *J* = 7.5, 1.4 Hz, 21H), 7.59-7.38 (m, 2H), 7.27 (s, 1H), 2.54 (s, 2H), 2.40 (d, *J* = 45.8 Hz, 2H), 2.40 (s, 1H); ^{13}C NMR (125 MHz, DMSO-d_6, δ ppm): 159.97 (s), 159.61 (s), 150.71 (s), 140.44 (s), 138.64 (s), 137.07 (s), 134.43 (s), 131.60 (s), 131.02 (s), 128.39 (s), 122.64 (s), 121.96 (s), 121.30 (s), 112.43 (s), 103.64 (s), 99.34 (s), 17.97 (s), 16.65 (s); MS: EIMS (*m/z*) 321 (M+1).

4-(2,5-Dimethylthiophen-3-yl)-6-(4-fluorophenyl)-pyrimidin-2-amine (4e7): Colour: pale yellow solid, yield: 82%, m.p.: 112-114 ºC; IR (KBr, ν_{max}, cm^{-1}): 787 (C–S), 1645 (C=C), 1376 (C–CH_3), 1608 (C=N), 3075 (NH_2), 1283 (C–F), 1242 (C–N); ^{1}H NMR (500 MHz, DMSO-d_6, δ ppm): 7.85-7.46 (m, 2H), 7.36 (s, 1H), 7.18 (dd, *J* = 15.2, 7.4 Hz, 3H), 2.52 (s, 2H), 2.46 (s, 3H), 2.39 (s, 3H). ^{13}C NMR: (125 MHz, DMSO-d_6, δ ppm): 165.57 (s), 163.47 (s), 160.68 (s), 158.34 (s), 155.97 (s), 140.44 (s), 138.64 (s), 132.26 (d, *J* = 3.7 Hz), 131.60 (s), 131.02 (s), 130.69 (d, *J* = 7.6 Hz), 116.08 (s), 115.86 (s), 107.58 (s), 17.97 (s), 16.65 (s); MS: EIMS (*m/z*) 300 (M+1).

4-(2,4-Difluorophenyl)-6-(2,5-dimethylthiophen-3-yl)-pyrimidin-2-amine (4f7): Colour: white solid, yield: 76%, m.p.: 310-312 ºC; IR (KBr, ν_{max}, cm^{-1}): 781 (C–S), 1540 (C=C), 1370 (C–CH_3), 1647 (C=N), 1213 (C–N), 3024 (NH_2), 823 (C–Cl); ^{1}H NMR (500 MHz, DMSO-d_6, δ ppm): 7.63 (dt, *J* = 7.2, 5.0 Hz, 1H), 7.33 (s, 1H), 7.30 (d, *J* = 29.5 Hz, 2H), 7.08-6.77 (m, 2H), 2.51 (s, 2H), 2.42 (s, 3H), 2.35 (s, 3H). ^{13}C NMR (125 MHz, DMSO-d_6, δ ppm): 166.73 (d, *J* = 6.7 Hz), 164.64 (d, *J* = 7.6 Hz), 164.11 (d, *J* = 6.7 Hz), 162.01 (d, *J* = 7.6 Hz), 158.59 (d, *J* = 6.7 Hz), 157.30 (s), 156.99 (s), 140.44 (s), 138.64 (s), 131.60 (s), 131.02 (s), 130.02 (t, *J* = 7.1 Hz), 121.74 (d, *J* = 3.7 Hz), 121.52 (d, *J* = 3.7 Hz), 113.19 (d, *J* = 3.7 Hz), 112.97 (d, *J* = 4.7 Hz), 110.96 (d, *J* = 3.7 Hz), 104.13 (s), 103.91 (s), 103.70 (s), 17.97 (s), 16.65 (s); MS: EIMS (*m/z*) 318 (M+1).

4-(2-Chlorophenyl)-6-(2,5-dimethylthiophen-3-yl)-pyrimidin-2-amine (4g7): Colour: white solid, yield: 78%, m.p.: 137-138 ºC; IR (KBr, ν_{max}, cm^{-1}): 756 (C–S), 1540 (C=C), 1370 (C–CH_3), 1647 (C=N), 1213 (C–N), 3024 (NH_2), 823 (C–Cl); ^{1}H NMR (500 MHz, DMSO-d_6, δ ppm): 7.93-7.53

(m, 1H), 7.53-6.95 (m, 5H), 7.25 (s, 1H), 7.25 (s, 1H), 2.51 (s, 2H), 2.43 (s, 3H), 2.34 (s, 3H); ^{13}C NMR (125 MHz, DMSO-d_6, δ ppm): 158.25 (s), 157.30 (s), 157.14 (s), 140.44 (s), 138.64 (s), 137.70 (s), 131.91 (s), 131.60 (s), 131.02 (s), 130.64 (s), 130.25 (s), 129.37 (s), 127.12 (s), 111.01 (s), 17.97 (s), 16.65 (s); MS: EIMS (*m/z*) 316 (M+1).

4-(2,4-Dichlorophenyl)-6-(2,5-dimethylthiophen-3-yl)-pyrimidin-2-amine (4h7): Colour: white solid, yield: 74%, m.p.: 148-150 ºC; IR (KBr, ν_{max}, cm^{-1}): 626 (C–S), 1647 (C=C), 1350 (C–CH_3), 1608 (C=N), 1274 (C–N), 3349 (NH_2), 874 (C–Cl), 3034 (C–H); ^{1}H NMR (500 MHz, DMSO-d_6, δ ppm): 7.54 (dd, *J* = 9.9, 4.5 Hz, 2H), 7.45-7.33 (m, 2H), 7.25 (s, 1H), 2.50 (s, 2H), 2.42 (s, 3H), 2.34 (s, 3H); ^{13}C NMR (125 MHz, DMSO-d_6, δ ppm): 158.25 (s), 157.30 (s), 157.14 (s), 140.44 (s), 138.64 (s), 135.34 (s), 134.24 (s), 133.82 (s), 131.60 (s), 131.09 (d, *J* = 16.2 Hz), 130.52 (s), 128.16 (s), 111.01 (s), 17.97 (s), 16.65 (s); MS: EIMS (*m/z*) 351 (M+1).

Pharmacological activity

Animal ethics: All experimental procedures involving mice were conducted in accordance with the guidelines of the Committee for the Purpose of Control and Supervision of Experiments on Animals (CPCSEA; Registration No. 1447/PO/Re/S/11/CPCSEA) and were approved by the Institutional Animal Ethics Committee (IAEC) of the Department of Pharmaceutical Sciences, TRR College of Pharmacy, Hyderabad, India.

Antidepressant activity: The *in vivo* antidepressant potential of the synthesized pyrimidine derivatives (**4e7** and **4h7**) was assessed using two validated behavioural paradigms–the Forced Swimming Test (FST) and the Tail Suspension Test (TST). The study utilized adult male Swiss albino mice (20 ± 4 g), a standard strain recommended for behavioural and psychopharmacological evaluations. The animals were procured from the institutional animal facility and acclimatized prior to experimentation. Animals were housed in polypropylene cages (six per cage) under controlled environmental conditions (12 h light/dark cycle, 22 ± 2 ºC, 55 ± 5% relative humidity) with ad libitum access to standard pellet diet and water. The mice were randomly allocated into six experimental groups (n = 6 per group) as: **Group I:** Vehicle control (0.5% aqueous Tween 80); **Group II:** Standard drug (imipramine, 20 mg/kg, intraperitoneally); **Groups III–VI**: Test compounds **4e7** and **4h7** respectively (each at 100 mg/kg, intraperitoneally).

The selected dose of 100 mg/kg for the test compounds was based on preliminary toxicity screening and the reported pharmacological ranges for similar scaffolds. Imipramine was served as the reference standard for comparing the antidepressant efficacy of the synthesized test compounds.

Acute oral toxicity was evaluated in accordance with the acute oral toxicity study was performed in accordance with the Organisation for Economic Co-operation and Development (OECD) Guideline 425, Up-and-Down Procedure). No mortality or significant behavioural changes were observed at the tested dose and the median lethal dose (LD_{50}) was estimated to be above 2000 mg/kg.

Behavioural analysis: Each animal was subjected to a single trial for both the Forced Swim Test and Tail Suspension Test to avoid habituation effects. All behavioural observations were recorded and scored by an investigator blinded to the treatment groups to ensure unbiased assessment.

Forced Swimming Test (FST) and Tail Suspension Test (TST) were conducted 30 min after administration of the test compounds or the reference drug. In the FST, each mouse was placed individually in a transparent glass cylinder containing water maintained at 25 ± 1 ºC (depth 15 cm) for 6 min and the immobility period was recorded during the final 4 min. In TST, mice were suspended by tail for 6 min, with immobility duration measured over last 4 min. A reduction in the immobility time was considered indicative of the antidepressant activity.

Data are presented as the mean ± standard error of mean (SEM). Statistical comparisons were carried out using the one-way analysis of variance (ANOVA) followed by the Dunnett's post hoc test to evaluate differences between the control and treatment groups. Differences were considered statistically significant at $p < 0.05$.

The dose of a 100 mg/kg selected for synthesized hybrid thiophene-pyrimidine derivatives (**4e7** and **4h7**) was based on literature reports of the similar heterocyclic scaffolds exhibitting antidepressant activity in rodents within the range. Prior to behavioural testing, acute oral toxicity studies were conducted following according to OECD Guideline No. 425 (Up-and-Down Procedure) and no mortality or significant behavioural changes were observed at doses up to the 2000 mg/kg, indicating favourable safety profile. Therefore, 100 mg/kg was been considered safe and pharmacologically relevant dose for initial screening. The intraperitoneal route was chosen to ensure reliable systemic absorption and minimize variability associated with the oral bioavailability. The test compounds were administered in 0.5% aqueous Tween 80, standard vehicle for *in vivo* studies. Imipramine, a clinically approved tricyclic antidepressant, were used as the reference drug at 20 mg/kg i.p., a well-established dose in animal models, allowing comparative evaluation of antidepressant potential of the test compounds.

Forced Swim Test (FST): For FST, mice were placed in a cylindrical glass (25 cm × 15 cm × 25 cm) filled with water to depth of 15 cm to evaluate their immobility behaviour. At 60 min post-oral administration of the test compounds, the mice were submerged in the water maintained at 24 ± 1 ºC for 4 min. During this period, the time spent immobile, latency to immobility, as well as frequency of climbing and swimming behaviours, were recorded. To minimize stress due to the handling, the first minute of test was excluded from observation. Imipramine was used as positive control, while distilled water served as the negative control. After test, animals gently removed from water, dried with towel and kept in warm environment until fully dry. Antidepressant-like the effects were inferred from longer latency to immobility and reduction in duration of immobility, while climbing and swimming behaviours were analyzed to explore potential mechanisms of action of compounds. The immobility time for each mouse was measured to evaluate antidepressant activity.

In behavioural tests, conventional antidepressants were found significantly reduce the immobility time, suggesting the antidepressant-like activity. Data analysis performed using one-way ANOVA, followed by Dunnett's post hoc test to

determine statistical significance between treatment and control groups. The percentage reduction in immobility duration (%DID) for each test compound and reference drug was been calculated using following equation:

$$\text{DID } (\%) = \left(\frac{(A - B)}{B}\right) \times 100$$

where A represents the immobility duration observed in the test group; and B represents the immobility duration observed in the control.

Tail Suspension Test (TST): The tail suspension test is widely used method for assessing immobility in the mice by suspending from the tail. In this study, a mark was made 1 cm from the tail tip and the procedure was performed 1 h after oral administration of the test compounds. Imipramine hydrochloride served as a positive control in this experiment. The mice were hung 50 cm above the ground by their tails and left suspended for a total duration of 4 min. The last 3 min of the suspension were monitored for specific behaviours, which included immobility time (defined as the absence of any active movement), swinging time (characterized by continuous paw movements in a vertical position while maintaining body alignment or moving side to side), curling time (active twisting movements of the body) and pedaling (continuous paw movements without body displacement). During the test, if any mouse attempted to climb its tail, it was gently repositioned to allow the procedure to continue.

Docking studies: In this study, interactions between a series of the synthetic hybrid thiophene-pyrimidine derivatives (**4a7-4h7**) and serotonin reuptake transporter (SERT) were examined through the rigid receptor docking and the computational docking simulations. The 3D structure of serotonin transporter (SERT) was retrieved from RCSB Protein Data Bank. (PDB ID: 1KUV, resolution 1.2 Å) and served as reference model. The structural integrity and suitability of selected protein for docking studies were assessed using the PROCHECK, which applies a nearest neighbour genetic algorithm (KNN-GA) to evaluate stereochemical quality and validate the molecular docking compatibility. Docking simulations were initially performed using the AutoDock 4.2. In protein preparation phase, all water molecules and heteroatoms removed, polar hydrogen atoms added and AD4-type atom parameters were assigned. The docking grid centered on the active site, which was defined using coordinates of co-crystallized ligand from original structure. Ligands were treated as flexible during docking, while receptor was kept rigid. Default Lamarckian genetic algorithm settings were used for all the docking runs. Further docking simulations and energy refinement were conducted using the AutoDock 4.2 to enhance accuracy of binding affinity predictions. Each ligand underwent 10,000 cycles energy minimization confined to active site cavity No 1. The primary binding pocket composed of key amino acid residues: GLY134A, GLY136A, GLN133A, LYS135A, SER137A, GLN132A, VAL126A, ARG131A, PHE167A, LEU164A, ALA163A, GLU161A and VAL59A. The docking outcomes, comprising binding affinity values and key interactions such as hydrogen bonds and π–π stacking.

Molecular dynamic simulations: Molecular dynamics (MD) simulations were carried out using GROMACS 2018 simulation package to evaluate the structural stability and dynamic behaviour of protein–ligand complexes involving serotonin reuptake transporter (SERT) and synthesized hybrid thiophene-pyrimidine derivatives. The CHARMM36 all-atom force field was employed to model the protein, while the ligand topologies and parameters were generated using the CGenFF server to ensure the force field compatibility. Each complex was then solvated in a triclinic box using the TIP3P explicit water model, with minimum distance of 1.0 nm between the protein surface and the box edges to avoid the edge effects. To neutralize system, appropriate counterions (Na^+ or Cl^-) added. Energy minimization was performed using steepest descent algorithm to eliminate the steric clashes and optimize the system's geometry. The system was equilibrated in two phases: initially under constant volume and temperature (NVT ensemble) for 100 picosec at 300 K using V-rescale thermostat, followed by the 100 picosec under constant pressure and the temperature (NPT ensemble) at 1 bar using Parrinello–Rahman barostat. After equilibration, a production run of 100 nanoseconds was conducted. Periodic boundary conditions were applied in all the directions. Electrostatic interactions were calculated using Particle Mesh Ewald (PME) method, with cut-off of 1.2 nm for both the electrostatic and van der Waals interactions. Bond lengths involving hydrogen atoms were constrained using LINCS algorithm. Post-simulation, trajectory analysis was performed to assess stability and flexibility of the protein–ligand complexes. Root mean square deviation (RMSD) was calculated to monitor overall conformational stability over time, while root mean square fluctuation (RMSF) was used to evaluate flexibility of individual amino acid residues. Solvent accessible surface area (SASA) analysis was conducted to determine extent of the protein's exposure to solvent.

RESULTS AND DISCUSSION

This study outlines the multistep synthesis of hybrid 2,5-dimethyl-thiophen-3-yl)pyrimidin-2-amine derivatives (**4a7-4h7**). Initially, 3-acetyl-2,5-dimethylthiophene when combined with aqueous KOH generated an enolate intermediate under basic condition. To this reactive mixture, an equimolar amount of respective aromatic aldehyde was added, initiated Claisen-Schmidt condensation reaction to yield **4a-h** derivatives. In the subsequent step, these intermediates **4a-4h** were reacted with guanidine hydrochloride to form the target derivatives (**4a7-4h7**). The products were obtained in satisfactory yields and purity, as confirmed by the TLC and melting point determination. The structural characterization was carried out using spectroscopic techniques. The ^{1}H NMR spectra of the synthesized derivatives displayed the characteristic signals, including a multiplet at δ 7.57-7.29 (m, 3H) corresponding to the CH_3-H proton of thiophene ring, a singlet at δ 7.26 ppm indicative of NH_2 group of pyrimidine ring supporting the proposed structure of 2,5-dimethylthiophen-3-yl)pyrimidin-2-amine derivatives. EI-MS of all the synthesized compounds showed [M + H] peaks consistent with the molecular masses.

Pharmacological activity: The antidepressant potential of compounds **4e7** and **4h7** was evaluated in mice using the Forced Swim Test (FST) and Tail Suspension Test (TST) at a

dose of 100 mg/kg, with imipramine (20 mg/kg) as reference standard. No mortality or notable behavioural alterations were observed in any treatment group. Toxicological assessment indicated that the compounds were well tolerated up to 2000 mg/kg body weight. A dose–response study using 25, 50, 100 and 200 mg/kg identified 100 mg/kg as the most effective dose and was used for further testing.

The results shown in Tables 1 and 2 revealed that imipramine reduced immobility time by 68.82% in both FST and TST. All synthesized compounds produced noticeable antidepressant-like effects, with **4e7** and **4h7** showing the most significant activity. Compound **4h7** reduced immobility by 60.2% in FST and 55.3% in TST, while compound **4e7** produced reductions of 55.2% in FST and 49.0% in TST. These outcomes suggest strong antidepressant potential for both compounds, with efficacy approaching that of imipramine.

The structure–activity relationship analysis supports these findings. The pyrimidine moiety in this hybrid derivatives (**4a7-4h7**) plays a key role in enhancing antidepressant activity through π–π stacking and hydrogen-bonding interactions with serotonin-related targets. This scaffold also improves binding stability, CNS penetration, lipophilicity and receptor affinity. Electron-donating groups on the pyrimidine ring further enhanced interactions with serotonin transporters, contributing to improved activity.

Docking studies: Docking simulations with the serotonin transporter (PDB: 1KUV) using Autodock 4.2 showed that all synthesized compounds had favourable AutoDock scores, with **4e7** and **4h7** being the strongest (Table-3). Compounds with lower docking scores showed higher energy requirements for binding. In compound **4h7**, the *ortho*, *para*-chloro substituent enabled NH bonding, SH bonding and pi-alkyl interactions with GLUA161, TYRA168, LEUA109, LEUA158, LEUA121 and PROA64. Compound **4e7** with a *para*-fluoro group, formed NH bonding, SH bonding, pi-alkyl and pi-pi interactions with GLUA161, TYRA68, LEUA158, LEUA121, PHEA188, PHEA56 and CYSA63 (Fig. 1).

Docking energies further supported the results, with **4e7** and **4h7** showing binding energies of –7.8 kcal/mol and –8.0 kcal/mol, comparable to imipramine (–9.1 kcal/mol). The presence of NH-bonding, SH-bonding, π–π and π-alkyl interactions with key residues such as GLUA161, TYRA168, LEUA121 and PHEA56 indicates strong and stable binding. Additional interactions with Tyr95, Phe341 and Asp98 further confirmed high affinity toward the SERT active site. These molecular interactions correlate well with *in vivo* findings and support that the antidepressant-like activity of compounds **4e7** and **4h7** is mediated through effective SERT inhibition.

Molecular dynamic studies: Molecule with the highest binding affinity is further subjected for molecular dynamic simulations.

RMSD: The standard complex (orange) fluctuates between 0.22–0.30 nm, with slight rise up to ~0.32–0.34 nm around 80 ns, indicating more conformational changes and less stability. The test compound complex (blue) remains more stable, with RMSD consistently in range of 0.15–0.25 nm, showing very minor deviations throughout simulation (Fig. 2). Lower RMSD values mean that the test ligand maintains the protein structure with fewer conformational shifts. The test compound shows a more stable binding profile compared to standard drug, suggesting that it forms tighter and more reliable complex with target protein, which is favourable for potential antidepressant activity.

To strengthen the MD simulation results, we have now included a quantitative summary data presenting the key dynamic parameters such as RMSD, RMSF, hydrogen bond occupancy and binding stability metrics for the ligand–protein complexes. Table-4 provides a consolidated view of structural fluctuations, flexibility of active-site residues and the stability of ligand interactions throughout the simulation. This quantitative representation supports the interpretation of the MD trajectory and further validates the stability of the docked complexes.

TABLE-1
FORCE SWIM METHOD RESULTS OF 2,5-DIMETHYLTHIOPHEN-3-YL)PYRIMIDIN-2-AMINE DERIVATIVES

Compound	Duration of immobility	Latency of immobility	Climbing period	Swimming period	% Decrease in immobility duration
4e7	44.8 ± 4.6	69.6 ± 2.9	35.5 ± 3.2	44.2 ± 3.0	55.2
4h7	39.8 ± 4.3	68.7 ± 3.0	37.8 ± 3.3	39.5 ± 3.3	60.2
Control	96.2 ± 4.2	12.5 ± 4.4	18.9 ± 4.2	28.6 ± 5.6	0
Std. (imipramine)	30.7 ± 5.0	68.8 ± 3.6	66.9 ± 4.8	20.8 ± 3.8	68.8

Values are expressed as mean ± SD (n = 6); One-way ANOVA followed by Tukey's test; ns = not significant, $p < 0.05$ significant, $p < 0.01$ very significant, $p < 0.001$ highly significant *vs*. control.

TABLE-2
TAIL SUSPENSION METHOD RESULTS OF 2,5-DIMETHYLTHIOPHEN-3-YL)PYRIMIDIN-2-AMINE DERIVATIVES

Compound	Duration of immobility	Swinging period	Curling period	Pedeling period	% Decrease in immobility duration
4e7	48.9 ± 3.2	50.6 ± 3.9	49.2 ± 3.8	32.5 ± 3.3	49.0
4h7	43.4 ± 3.8	52.4 ± 3.6	50.4 ± 4.2	29.4 ± 4.2	55.3
Control	96.2 ± 4.2	12.5 ± 4.4	18.9 ± 4.2	28.6 ± 5.6	0
Std. (imipramine)	30.7 ± 5.0	68.8 ± 3.6	66.9 ± 4.8	20.8 ± 3.8	68.8

Values are expressed as mean ± SD (n = 6); One-way ANOVA followed by Tukey's test; ns = not significant, $p < 0.05$ significant, $p < 0.01$ very significant, $p < 0.001$ highly significant *vs*. control.

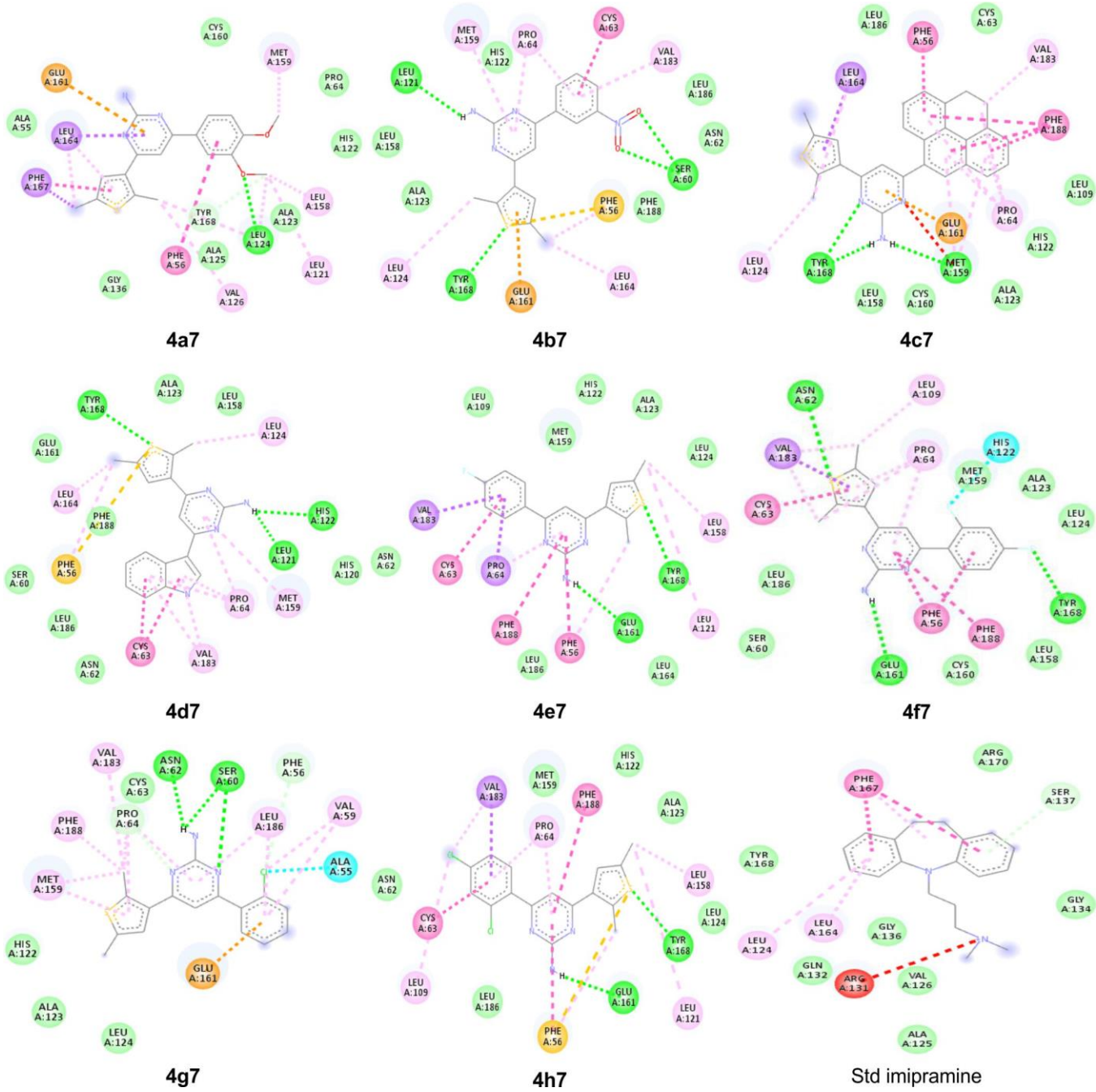

Fig. 1. Docking poses with 1KUV

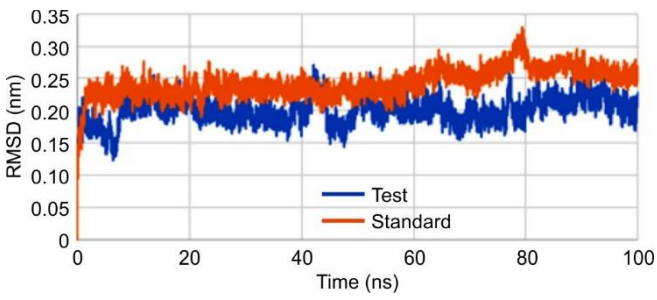

Fig. 2. RMSD

RMSF: Overall, both complexes show fluctuations mostly between 0.1–0.3 nm, which indicates stable binding across the protein. The standard drug (orange) shows higher flexibility around residues 50-70 (peak ~0.50-0.55 nm) again at residues 150-160 (~0.45-0.50 nm). The test compound (blue) maintains lower fluctuations across most regions, generally ~0.1–0.25 nm, smaller peaks near residues 30-60 (~0.30-0.35 nm) and at the terminal region (~0.4 nm). Importantly, in the central core region (80–130 residues), test ligand shows much lower fluctuations (< 0.2 nm) compared to standard, indicating stronger and more stable interactions (Fig. 3). The RMSF results demonstrate that test compound stabilizes the protein more effectively than standard, with lower residue fluctuations in core binding region, supporting its potential as more reliable antidepressant candidate.

TABLE-3
DOCKING SCORES OF COMPOUNDS SHOWING THE ANTIDEPRESSANT ACTIVITY AGAINST 1KUV

Compound	Amino acid residues	Interactions	Glide score (Kcal/mol)
4a7	LEUA 124 LEUA 158, LEUA 121, VALA 126, META 159 PHEA 56	H-bonding Pi-alkyl Pi-Pi	-7.6
4b7	LEUA 121 TYRA 168 SERA 160	NH bonding SH bonding H-bonding	-6.6
4c7	MET159, TYR 168 LEUA 124, VALA183.PROA164 PHEA158, PHEA56	NH bonding Pi-alkyl Pi-Pi	-6.8
4d7	HISA122, LEUA121, TYRA168 CYSA63 PHEA56	H-bonding Pi-Pi SH bonding	-7.5
4e7	GLUA161 TYRA68 LEUA158, LEUA121 PHEA188, PHEA56, CYSA63	NH bonding SH bonding Pi-alkyl Pi-Pi	-7.8
4f7	TYRA168 GLUA161 PHEA56, PHEA188, CYSA63	H-bonding NH bonding Pi-Pi	-7.2
4g7	ASNA62, SERA60 ALAA59, LEUA186, PHEA188, META159	NH bonding Pi-alkyl	-7.0
4h7	GLUA161 TYRA168 LEUA109, LEUA158, LEUA121, PROA64	NH bonding SH bonding Pi-alkyl	-8.0
Std. (imipramine)	PHEA167 LEUA124, LEUA164	Pi-Pi Pi-alkyl	-9.1

TABLE-4
SUMMARY OF MD SIMULATION PARAMETERS

Parameter	Standard complex	Test complex
RMSD (nm)	0.22-0.30 nm; rises to ~0.32-0.34 nm	0.15-0.25 nm (more stable)
RMSF (nm)	Higher fluctuations at residues 50-70 and 150-160	Lower fluctuations across residues; < 0.2 nm in core region
Conformational stability	More conformational changes	Stable throughout simulation
Residue flexibility	Higher flexibility	Lower flexibility
Overall binding stability	Moderate	Strong and stable

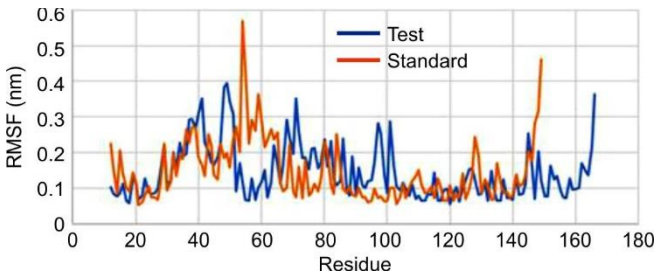

Fig. 3. RMSF

Conclusion

The synthesis of new series of (2,5-dimethylthiophen-3-yl)-pyrimidin-2-amine derivatives (**4a7**-**4h7**) was successfully achieved. The compounds were synthesized *via* Claisen–Schmidt condensation followed by the cyclization with guanidine hydrochloride. Structural confirmation was achieved through ^{1}H NMR, ESI-MS and CHN analyses, which supported the proposed molecular structures. Pharmacological screening using Forced Swim Test (FST) and Tail Suspension Test (TST) demonstrated that all compounds exhibited antidepressant activity, with compounds **4e7** and **4h7** showing the most pronounced effects. These compounds significantly reduced immobility times, with efficacy comparable to standard drug imipramine and were found to be safe up to 2000 mg/kg body weight. Docking studies against the serotonin transporter (PDB ID: 1KUV) revealed strong binding affinities for compounds **4e7** and **4h7**, attributed to hydrogen-bonding and π–π interactions with key amino acid residues. The presence of electron donating and halogen substituents on pyrimidine ring enhanced receptor affinity and lipophilicity, correlating with observed biological activity. Overall, the integrated experimental and computational results indicate that halogen-substituted pyrimidine derivatives, particularly compounds **4e7** and **4h7**, possess potent antidepressant potential and could serve as a promising lead candidate for further development.

ACKNOWLEDGEMENTS

The authors sincerely acknowledge the management of Sri Padmavati Mahila Visvavidyalayam, Institute of Pharmaceutical Sciences, Tirupati, India and TRR College of

Pharmacy, Hyderabad India, for extending the facilities and support essential for the successful completion of this research work.

CONFLICT OF INTEREST

The authors declare that there is no conflict of interests regarding the publication of this article.

REFERENCES

1. K.N. Venugopala and V. Kamat, *Pharmaceuticals*, **17**, 1258 (2024); https://doi.org/10.3390/ph17101258
2. 2. S. Kumar and B. Narasimhan, *Chem. Centr. J.*, **12**, 38 (2018); https://doi.org/10.1186/s13065-018-0406-5
3. S.B. Patil, *Heliyon*, **9**, e16773 (2023); https://doi.org/10.1016/j.heliyon.2023.e16773
4. A. Mahapatra, T. Prasad and T. Sharma, *Future J. Pharm. Sci.*, **7**, 123 (2021); https://doi.org/10.1186/s43094-021-00274-8
5. S.M. Sondhi, N. Singh, M. Johar and A. Kumar, *Bioorg. Med. Chem.*, **13**, 6158 (2005); https://doi.org/10.1016/j.bmc.2005.06.063
6. M.S. Mohamed, S.M. Awad and A.I. Sayed, *Eur. J. Med. Chem.*, **15**, 1882 (2009); https://doi.org/10.3390/molecules15031882
7. N. Ingarsal, G. Saravanan, P. Amutha and S. Nagarajan, *Eur. J. Med. Chem.*, **42**, 517 (2007); https://doi.org/10.1016/j.ejmech.2006.09.012
8. X.L. Zhao, Y.F. Zhao, S.C. Guo, H.S. Song, D. Wang and P. Gong, *Molecules*, **12**, 1136 (2007); https://doi.org/10.3390/12051136
9. K. Singh and T. Kaur, *MedChemComm*, **7**, 749 (2016); https://doi.org/10.1039/C6MD00084C
10. S.A. Abdel-Aziz, M.A. Hussein and I.T. Abdel-Raheem, *Bull. Pharm. Sci.*, **34**, 149 (2011); https://doi.org/10.21608/bfsa.2011.63262
11. M. Dumbare, L. Kawale, V. Nade and R. Deshmukh, *Res. J. Pharm.*, **8**, 12 (2018); https://doi.org/10.7897/2230-8407.0812245
12. N.E.A. Abd El-Sattar, E.H.K. Badawy and M.S.A. Abdel-Mottaleb, *J. Chem.*, **2018**, 8795061 (2018); https://doi.org/10.1155/2018/8795061.
13. J.A. Coleman, E.M. Green and E. Gouaux, *Nature*, **532**, 334 (2016); https://doi.org/10.1038/nature17629
14. S. Majeed, A.B. Ahmad, U. Sehar and E.R. Georgieva, *Membranes*, **11**, 685 (2021); https://doi.org/10.3390/membranes11090685
15. A. Jadhav, S.G. Shingade, P.G. Dessai, B.S. Biradar and S. MamleDesai, *Curr. Drug Discov. Technol.*, **21**, 64 (2024); https://doi.org/10.2174/0115701638243835230925161546
16. M. Krol, G. Ślifirski, J. Kleps, S. Ulenberg, M. Belka, T. Bączek, A. Siwek, K. Stachowicz, B. Szewczyk, G. Nowak, B. Duszyńska and F. Herold, *Int. J. Mol. Sci.*, **22**, 2329 (2021); https://doi.org/10.3390/ijms22052329
17. I. Khan, M.A. Tantray, H. Hamid, M.S. Alam, A. Kalam, F. Hussain and A. Dhulap, *Bioorg. Chem.*, **68**, 41 (2016); https://doi.org/10.1016/j.bioorg.2016.07.007
18. B. Mathew, J. Suresh and S. Anbazhagan, *J. Saudi Chem. Soc.*, **20**, S132 (2016); https://doi.org/10.1016/j.jscs.2012.09.015
19. S.B. Wang, X.Q. Deng, Y. Zheng, Y.P. Yuan, Z.S. Quan and L.P. Guan, *Eur. J. Med. Chem.*, **56**, 139 (2012); https://doi.org/10.1016/j.ejmech.2012.08.027
20. M.D. Lebar, K.N. Hahn, T. Mutka, P. Maignan, J.B. McClintock, C.D. Amsler, A. van Olphen, D.E. Kyle and B.J. Baker, *Bioorg. Med. Chem.*, **19**, 5756 (2011); https://doi.org/10.1016/j.bmc.2011.08.033
21. S.A. Khan, A.M. Asiri, K.A. Alamry, S.A. El-daly and M.A.M. Zayed, *Russ. J. Bioorganic Chem.*, **39**, 312 (2013); https://doi.org/10.1134/S1068162013030072
22. E.H.A. El-All, N.A. Osman, A.M. El-Mahmoudy and A.N. Hassan, *Asian J. Pharm. Clin. Res.*, **9**, 306 (2016).
23. S.A. Khan and A.M. Asiri, *Arab. J. Chem.*, **10(Suppl. 2)**, S2890 (2017); https://doi.org/10.1016/j.arabjc.2013.11.018